Journal of Physics: Conference Series

PAPER • OPEN ACCESS

Wing Kinematics and Dynamics during Takeoff in Honeybees

To cite this article: Biao Yang *et al* 2024 *J. Phys.: Conf. Ser.* **2694** 012011

Wing Kinematics and Dynamics during Takeoff in Honeybees

Biao Yang[1], Yizhe Li[1,2], Zhanzhou Hao[3,4], Bo Yin[3,4], Ling Yin[1,5] and Jialei Song[1,5]*

[1]School of Mechanical Engineering, Dongguan University of Technology, Dongguan 523808, Guangdong, China
[2]College of Mechatronics and Control Engineering, Shenzhen University, Shenzhen 518060, Guangdong, China
[3]University of Chinese Academy of Sciences, Beijing 101408, China
[4]Institute of Mechanics, Chinese Academy of Sciences, Beijing 100190, China
[5]Guangdong Provincial Key Laboratory of Intelligent Disaster Prevention and Emergency Technology, Dongguan University of Technology, Dongguan, China
*Correspondence: songjl@dgut.edu.cn

Abstract. In this paper, we utilized an array of four high-speed cameras to capture intricate wing kinematics, allowing us to calculate flapping amplitudes, frequencies, wingtip velocities, the ratio of upstroke to downstroke duration, and the angles between the forewings and hindwings. Preliminary analysis revealed that bees typically perform at least 15 wingbeats before taking off, with wing stroke amplitudes exceeding 100 degrees and frequencies within the range of 220 to 260 Hz. Additionally, the maximum angle between the forewings and hindwings generally surpasses 50 degrees. The kinematic parameters of takeoff are distinctive, and the relationships among various kinematic parameters are presented in this paper. Of particular note is the variation in the angle between the forewings and hindwings, which increases and then decreases with changing wingbeat speeds. In addition, we reconstructed the kinematic model of the wing motion for computational fluid dynamics (CFD) simulation, which will further reveal the aerodynamic mechanisms involved.
Keywords. Flapping wing; honeybee; takeoff; kinematics; fluid dynamics.

1. Introduction

In the previous study of the mechanism of lift production on insects, the wing model is generally assumed as a rigid flat plate, which can capture the primary force characteristics. However, insect wings are flexible, and they can deform significantly away from the rigid plate during flapping. Due to the distribution of wing veins and thickness changes of folds, the deformation of insect wings is mainly torsion in the spanwise direction and curvature in the chord direction [1, 2]. Due to the anisotropy of the wings, the bending stiffness in the spanwise direction is 1-2 orders of magnitude greater than that in the chord direction [3]. Meng et al. studied the effects of torsion and curvature deformation on aerodynamics [4] and found that curvature increases lift and drag, while torsion has little effect on aerodynamics. The chord bending is mainly due to the fact that the forewing and hindwing are not integrated but coupled. The wing coupling mechanism is a cuticle attachment device on the wings of four winged insects [5], which connects the forewing and hindwing to a coupling unit to synchronize their flapping movements. Up to now, researchers have mainly focused on the morphology and material distribution of coupling mechanisms. On the basis of these two aspects, the functional principle of effectively maintaining the synchronization of locking and forewing and hindwing movements during insect flight was elucidated [6-12]. However, there is limited research on the impact of changes in the angle between the forewing and hindwing on aerodynamics. Ma et al. used a high-speed camera to capture the hovering flight of a bee, simply observing the angle changes between the forewing and hindwing during the flapping [13]. The calculation model used was two-dimensional, and it was found that the angle changes of the flexible model led to an increase in lift and drag, and the rate of drag increase was higher. Therefore, in order to further deepen the understanding and understanding of the mechanism of bee flapping motion and forewing and hindwing coupling motion, this study used four high-speed cameras to capture the takeoff motion of bees, and analyzed the flapping process and forewing and hindwing coupling of bees from a kinematic perspective under higher measurement accuracy conditions. Then CFD was used to calculate and analyze the dynamics of the reconstructed bee model.

2. Methods

2.1. Experimental Materials and Equipment

The flight measurements were carried out in a transparent acrylic viewing chamber with a 30cm edge. The captured bees enter the box through a clear catheter and begin flying after reaching an exit point for the catheter in the observation chamber. Measurements were taken at this juncture. Four high-speed cameras (Phantom VEO640L, manufactured by Vision Research, USA) were employed to record the bee takeoff process. These cameras were strategically positioned above the observation chamber as illustrated in the figure 1.

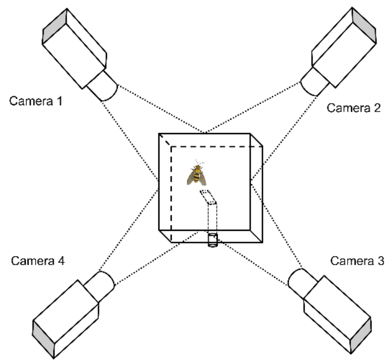

Figure 1. Four high-speed cameras and the location of the observation region.

2.2. Wing Motion Reconstruction

Five markers placed on the wings, as indicated in the figure 2(a), were utilized to characterize wing motion. These markers included the wing root, leading edge, wingtip, trailing edge, and the juncture between the forewing and hindwing. Moreover, we defined the Euler angles of wing motion. The Euler angles for wing motion, denoted as ϕ (stroke angle), θ (deviation angle), and ψ (pitch angle), were then calculated in the sequence mentioned to determine the position of the forewing, as illustrated in the figure 2(b).

(a) (b)

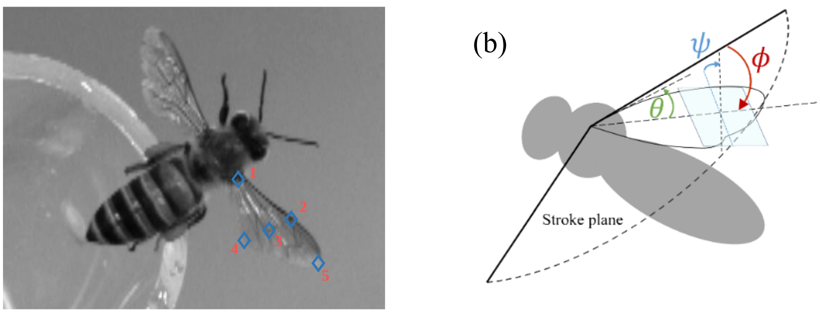

Figure 2. (a) Five tracking points on bee wings. (b) Definition of Euler angles for wing motion.

3. Results

3.1. Wing Kinematics during Takeoff in Honeybees

3.1.1. General Parameters. As shown in figure 3, the absolute values of wingbeat frequencies exhibited substantial differences within each takeoff sequence. Comparatively, differences in flapping amplitude were relatively smaller among different flight sequences than wingbeat frequency.

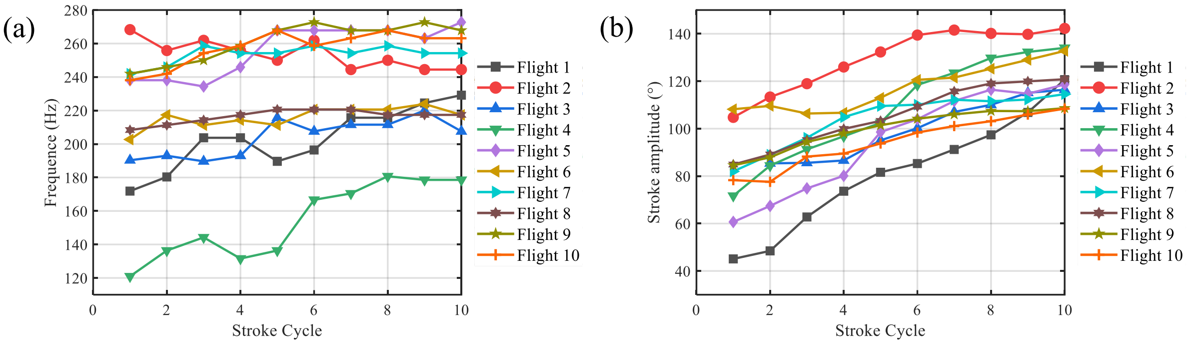

Figure 3. (a) The variation of wingbeat frequency. (b) The variation of flapping amplitude.

Wingbeat frequency and flapping amplitude are crucial in influencing the average wingtip velocity, as the square of wingtip velocity is directly proportional to aerodynamic forces. This relationship is typically expressed as 2ΦnR, where Φ represents flapping amplitude, n stands for wingbeat frequency, and R is the wingtip's flapping radius. We calculated the arithmetic mean of the wingtip speed for each cycle, as shown in figure 4(a). The figure 4(b) displays the relationship between wingbeat frequency, flapping amplitude and wingtip velocity for all cycles in the ten flight sequences. It is apparent from the figure that, as flapping amplitude increases, wingtip velocity also increases, while an increase in frequency does not significantly impact wingtip velocity. Therefore, we can conclude that during the takeoff process, changes in wingtip average velocity are primarily influenced by variations in flapping amplitude.

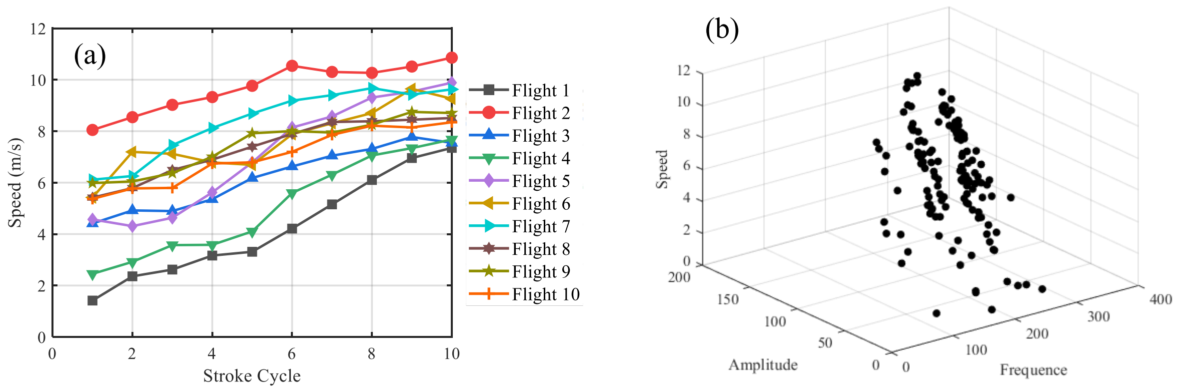

Figure 4. (a) The variation in wingtip average velocity over the wingbeat cycles. (b) The relationships between wingtip average velocity, wingbeat frequency, and flapping amplitude.

3.1.2. The Angle between Forewing and Hindwing. We calculated the angle between forewing and hindwing and express it as Δ. Figure 5 illustrates the changes in the Δ, as well as schematic representations of the Δ during the downstroke and upstroke phases. The Δ undergoes cyclical variations over time. For a single wingbeat cycle, during the upstroke phase, the angle increases to its maximum, then decreases, exhibiting a rebound effect.

Over the entire takeoff process, the maximum convexity of each cycle gradually increases, while the maximum concavity decreases. Similar to the analysis of the stroke angle, the angular difference between the maximum convexity and maximum concavity within one cycle is defined as the amplitude of the Δ. Our calculations reveal substantial differences in the amplitude of the Δ among various takeoff processes (as shown in figure 6). The maximum amplitude exceeds 170°, while the minimum is only 40°. Comparing the amplitude of the Δ with the average wingtip velocity for each flight, we find that the amplitude of Δ varies significantly and is entirely distinct from the trend of the average wingtip velocity. In most flights, the amplitude of the Δ increases first, then decreases. The flight with the greatest amplitude of the winglet angle does not necessarily correspond to the highest average wingtip velocity.

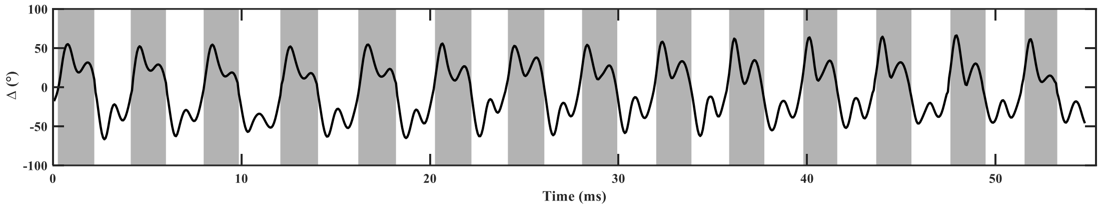

Figure 5. The temporal variations in the angle between forewing and hindwing.

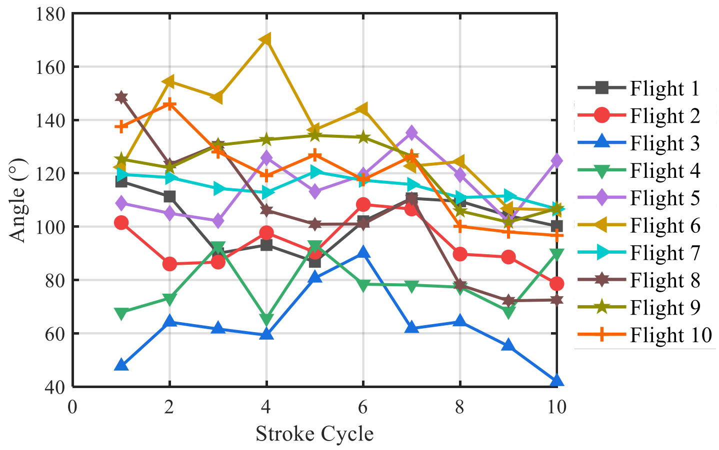

Figure 6. The amplitude of the angle between the forewing and hindwing varies with the wingbeat cycle.

3.1.3. Impact of Changes in the Angle between Forewing and Hindwing on Flight. Figure 7 shows the simplified chord profile of the wing under two wing beat modes, illustrating the variation in the angle of attack and the Δ changes during the upstroke and downstroke of honeybees. When the Δ is greater than zero, the wings exhibit positive flexion, which enhances the lift coefficient and delays the maximum stall angle. Although the calculated angle between forewing and hindwing during the upstroke is negative (indicating negative flexion), the wings maintain positive angles relative to the incoming airflow velocity during both the downstroke and upstroke. This strategy is evidently advantageous in terms of aerodynamics. Figure 8 displays the distribution of the Δ changes with respect to wingtip average velocity. It is observed that with increasing wingtip average velocity, the Δ initially increases before decreasing. This suggests that at lower speeds, greater wing flexion is favorable for increasing flapping speed, but as velocity increases further, the enhanced wing flexion results in higher drag. Thus, a reduction in wing flexion becomes necessary.

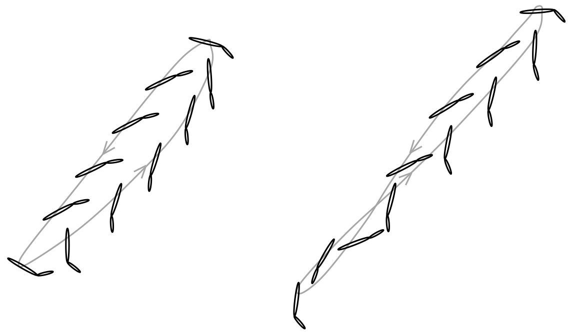

Figure 7. Simplified wing chordwise profile in two types of wingtip trajectories.

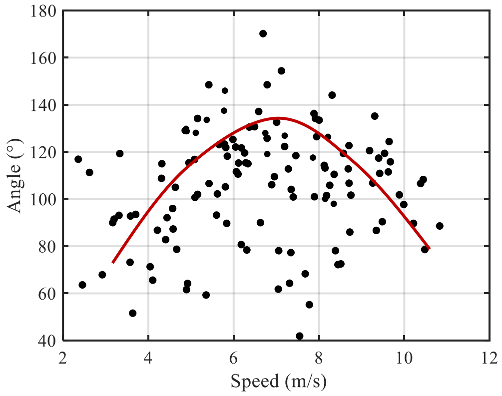

Figure 8. The variation of the angle between the forewing and hindwing with the wingtip average velocity.

3.2. Wing Dynamics during Takeoff in Honeybees

3.2.1. Simulation Setup. After the kinematics study, we also used the experimental data obtained before to carry out the numerical simulation of the dynamics on the computer. As shown in figure 9, two kinds of rigid wings were reconstructed on the basis of the original bee model, namely rigid wing Rigid_V1 with "Normal_1" as normal vector and rigid wing Rigid_V2 with "Normal_2" as normal vector. The following CFD calculations are based on rigid wings Rigid_V1,Rigid_V2 and the wings consisting of forewing and hindwing.

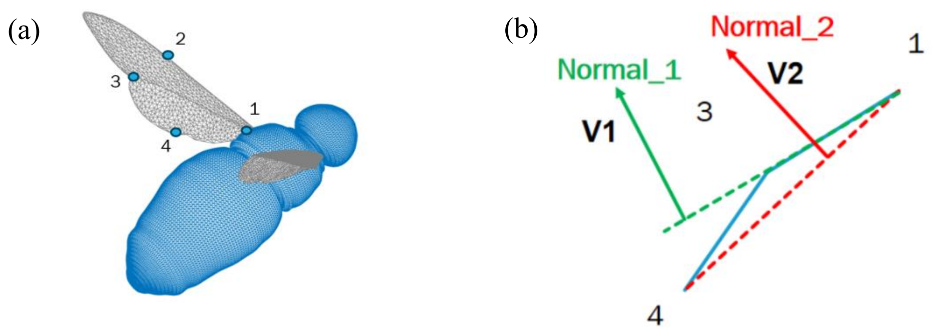

Figure 9. (a) The model of a bee. (b) The reconstruction of two rigid wings.

3.2.2. Different Wings Produce Different Lift and Thrust Forces. We used in-house CFD code based on finite-difference-immersed boundary method to calculate the average lift and thrust generated by the three wings in each cycle respectively. As shown in figure 10(a), the lift generated by Rigid_V1 is the largest among the three wings, while the lift generated by the Fore-Hind wing is the smallest. As shown in figure 10(b), the thrust generated by the Fore-Hind wing was the largest of the three wings, while the thrust generated by the Rigid_V1 was the smallest. Therefore, we can conclude that the wings shaped like Rigid_V1 are better for the bees to take off, while the wings shaped like Fore-Hind wing are better for the bees to fly quickly and control the body, so as to ensure the flexibility of flight.

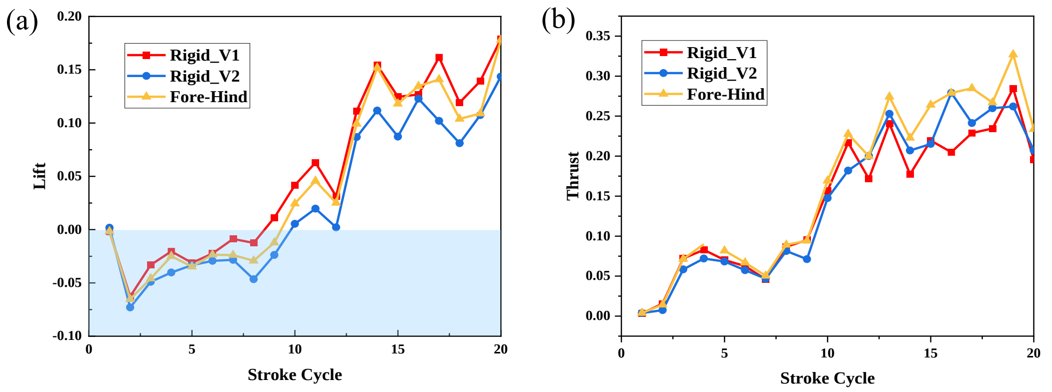

Figure 10. (a) The lift produced by the three wings. (b) The thrust produced by the three wings.

3.2.3. Different Wings Produce Different Air Flow Fields. In the simulation, we calculate the state of the air flow field around three different wing flapping. The study found that the vortices produced by the three wings were slightly different. As shown in figure 11, the Rigid_V1 wing produced the strongest leading edge vorticity (LEV), while the fore and hind wing produced the strongest spanwise vorticity.

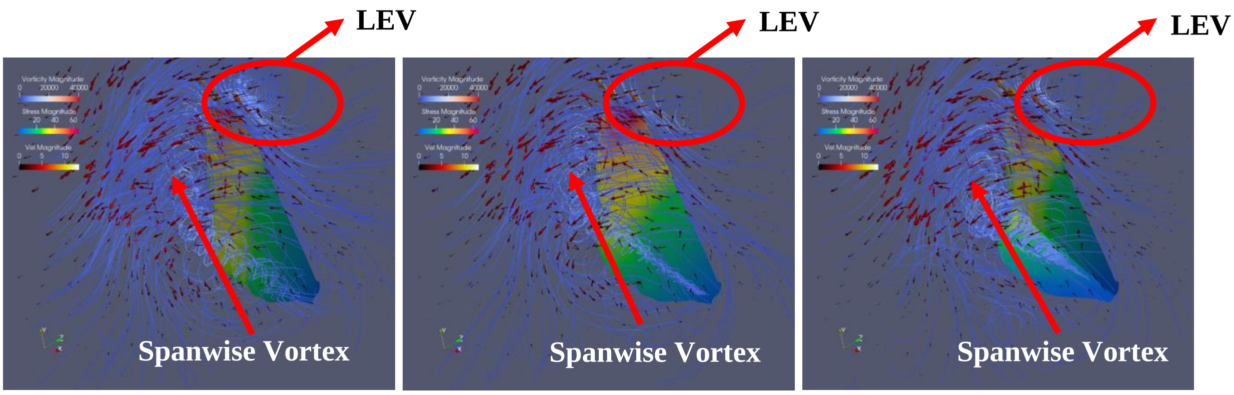

(a) (b) (c)

Figure 11. (a) The simulation calculation of Rigid_V1 wing. (b) The simulation calculation of Rigid_V2 wing. (c) The simulation calculation of Fore-Hind wing.

4. Conclusion

This study employed four high-speed cameras to capture the kinematics of honeybees during takeoff process, subsequently establishing a motion model for honeybee takeoff. Through kinematic analysis, this research focused on wing motion during the takeoff of honeybees. During the takeoff process, the variation in wingtip average velocity is predominantly influenced by wingbeat amplitude, with wingbeat frequency having a relatively minor impact. As for the changes in the angle between forewing and hindwing during takeoff, an increase in wingtip average velocity leads to an initial increase followed by a decrease in the angle between forewing and hindwing. This observation suggests that at lower speeds, higher wing flexion is advantageous for increasing wingbeat speed. Conversely, as velocity increases, a reduction in wing flexion becomes necessary. In the study of dynamics, we use the reconstructed bee motion model to carry out hydrodynamic simulation. Through calculation, we found that Rigid_V1 wing can produce stronger lift while Fore-Hind wing can produce stronger thrust during flight. The Rigid_V1 wing produced stronger leading edge vorticity, while the Fore-Hind wing produced stronger spanwise vorticity. In the follow-up study, PIV equipment will be used to conduct further experiments to verify the findings and conclusions of this paper in the air flow field, and further explore the laws and phenomena contained in the take-off process of honeybees.

Reference

[1] Ennos A R 1989 The kinematics and aerodynamics of the free flight of some Diptera *Journal of Experimental Biology* **142**(1) 49-85.
[2] Walker S M, Thomas A L R and Taylor G K 2010 Deformable wing kinematics in free-flying hoverflies *Journal of the Royal Society Interface* **7**(42) 131-142.
[3] Chari N, Prasad M and Laxminarayana P 2021 *Biophysics of Insect Flight* Springer.
[4] Meng X G and Sun M 2013 Aerodynamic effects of wing corrugation at gliding flight at low Reynolds numbers *Physics of Fluids* **25**(7) 071905.
[5] Gorb S 2001 *Attachment Devices of Insect Cuticle* Springer Science & Business Media.
[6] Scoble M J 1992 *The Lepidoptera, Form, Function and Diversity* Oxford University Press.
[7] Gorb S N and Goodwyn P J P 2003 Wing-locking mechanisms in aquatic Heteroptera *Journal of Morphology* **257**(2) 127-146.
[8] Perez G P J and Gorb S N 2004 Frictional properties of contacting surfaces in the hemelytra-hindwing locking mechanism in the bug Coreus marginatus (Heteroptera, Coreidae) *Journal of Comparative Physiology A* **190** 575-580.
[9] Stocks I C 2010 Comparative and functional morphology of wing coupling structures in Trichoptera: Annulipalpia *Journal of Morphology* **271**(2) 152-168.
[10] Ma Y, Ning J G, Ren H L, et al. 2015 The function of resilin in honeybee wings *The Journal of Experimental Biology* **218**(13) 2136-2142.
[11] Ma Y, Ren H, Ning J, et al. 2017 Functional morphology and bending characteristics of the honeybee forewing *Journal of Bionic Engineering* **14**(1) 111-118.
[12] Ogawa N and Yoshizawa K 2018 Structure and evolution of the stigmapophysis—A unique repose wing-coupling structure in Psocodea *Arthropod Structure & Development* **47**(4) 416-422.
[13] Ma Y, Ren H, Rajabi H, et al. 2019 Structure, properties and functions of the forewing-hindwing coupling of honeybees *Journal of Insect Physiology* **118** 103936.